

Switchable selectivity to electrocatalytic reduction of furfural over Cu₂O-derived nanowire arrays

Li Ma, Huiling Liu*, and Cheng Wang*

Affiliations:

Tianjin Key Laboratory of Advanced Functional Porous Materials and Center for Electron Microscopy, Institute for New Energy Materials & Low-Carbon Technologies, School of Materials Science and Engineering, Tianjin University of Technology, Tianjin 300384, China.

E-mail: hliu_tjut2016@163.com; cwang@tjut.edu.cn

Supplementary Results

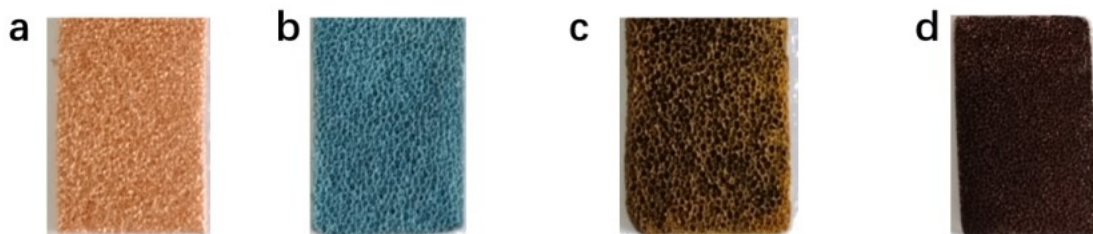


Fig. S1 Digital photographs of (a) Cu foam, (b) Cu(OH)₂ arrays, (c) Cu₂O arrays and (d) Cu₂O-D arrays.

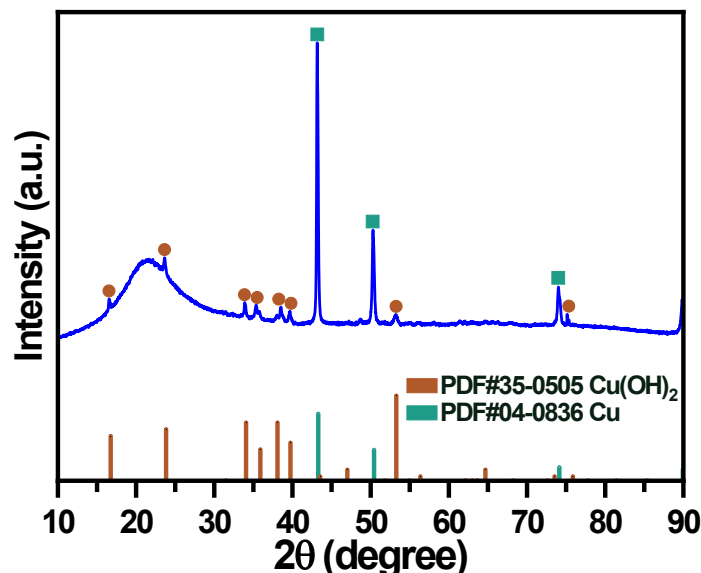


Fig. S2 XRD pattern of the Cu(OH)₂ arrays.

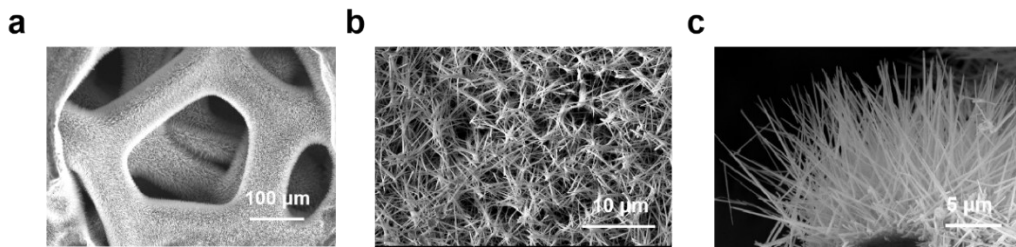


Fig. S3 SEM images of the $\text{Cu}(\text{OH})_2$ arrays.

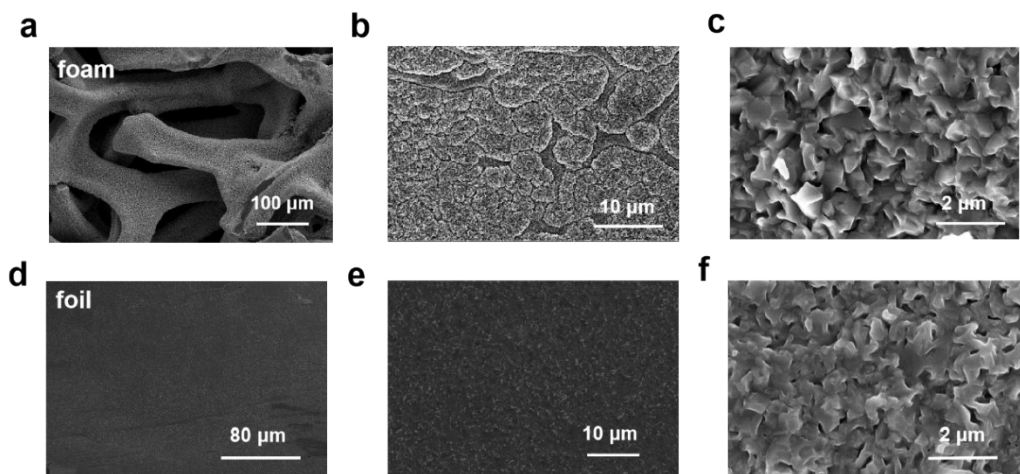


Fig. S4 SEM images of (a-c) Cu_2O foam, and (d-f) Cu_2O foil.

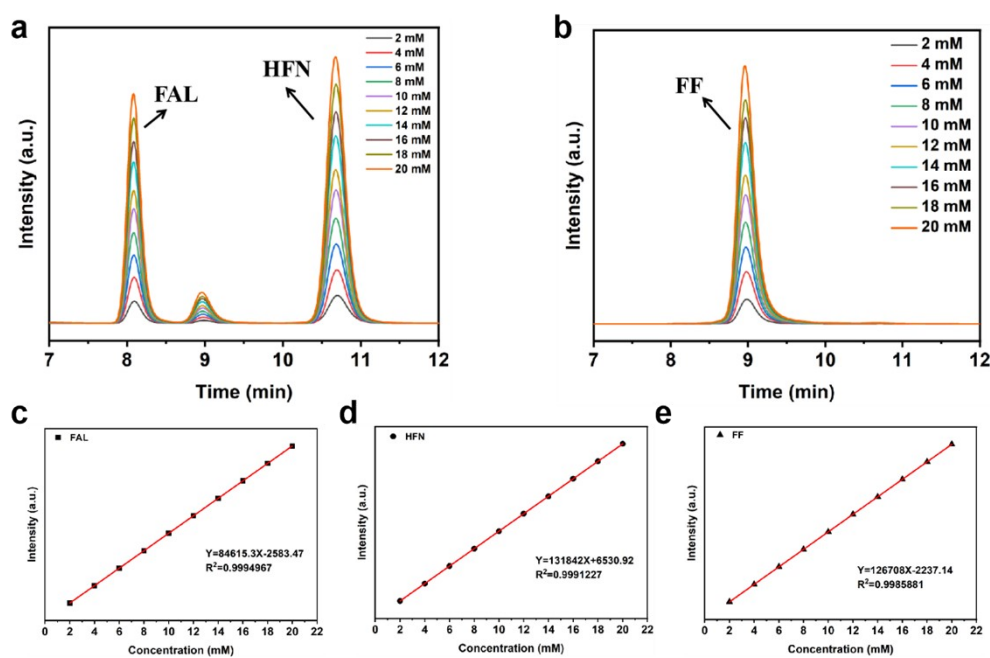


Fig. S5 Reference HPLC spectra for (a) FAL and HFN under UV absorption wavelength of 210 nm and (b) FF under UV absorption wavelength of 265 nm. Calibration curves of (c) FAL, (d) HFN and (e) FF.

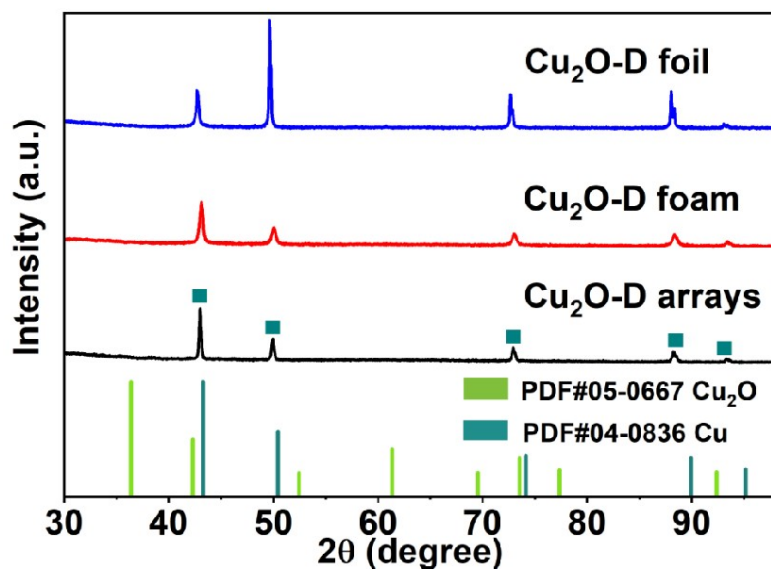


Fig. S6 XRD patterns of the Cu₂O-D arrays, Cu₂O-D foam and Cu₂O-D foil with electrochemical pretreatment.

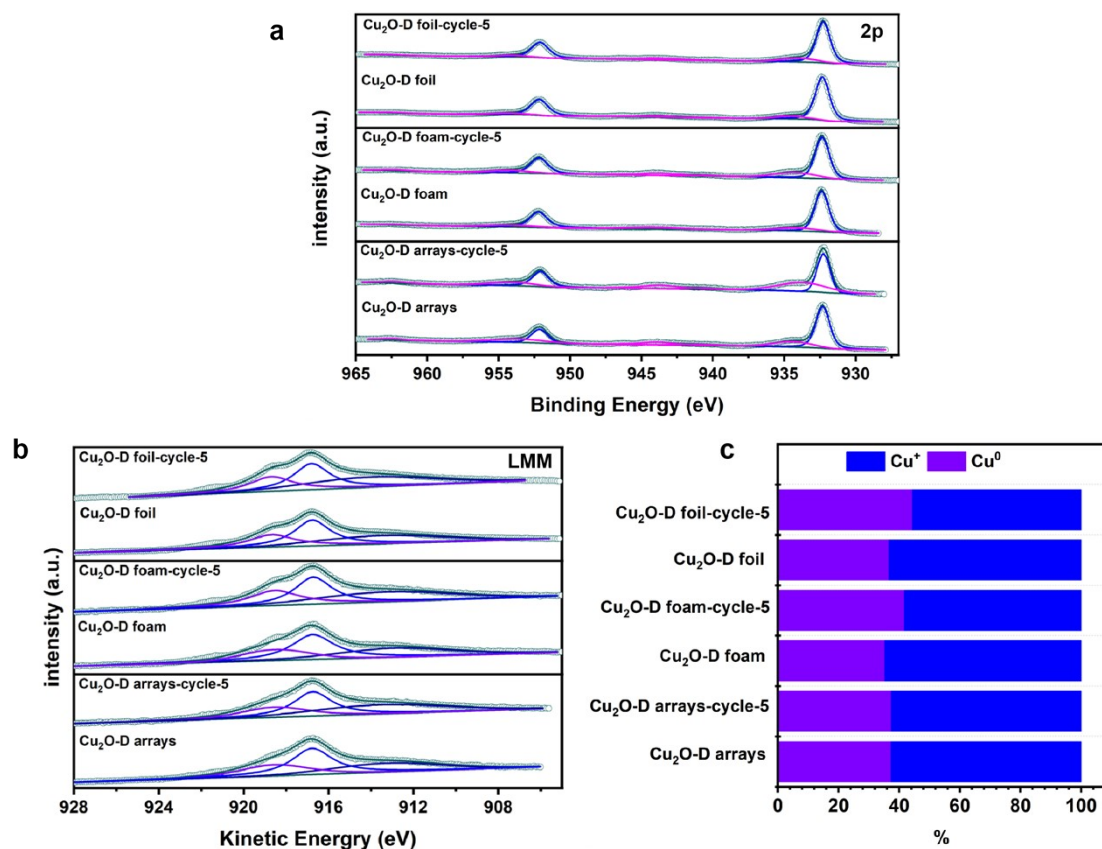


Fig. S7. (a) Cu 2p XPS spectra, (b) Auger Cu LMM and (c) relative percentage of Cu⁺ and Cu⁰ in the Cu₂O-D samples after electrocatalytic reduction of FF for five cycles.

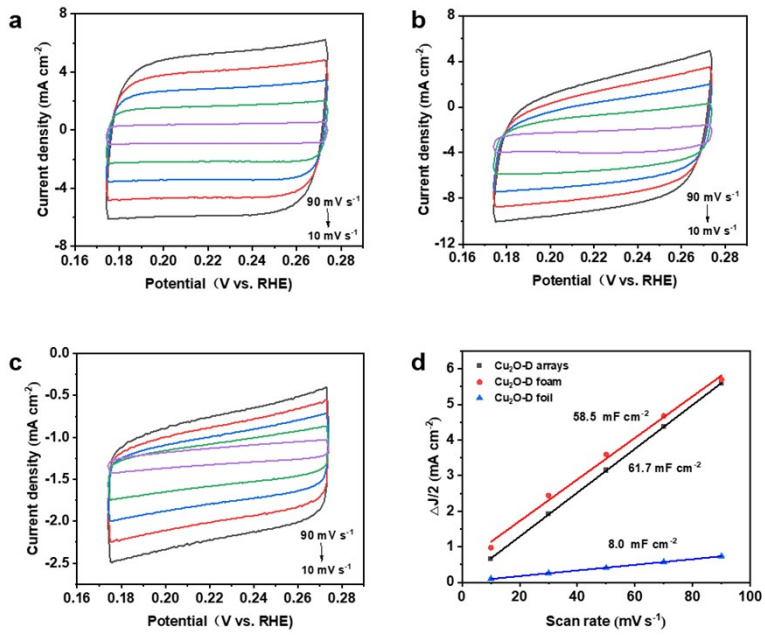


Fig. S8 CV curves of (a) Cu_2O -D arrays, (b) Cu_2O -D foam and (c) Cu_2O -D foil recorded at 0.17–0.27 V_{RHE} with sweep rates from 10 to 90 mV s⁻¹ in pH 14. (d) Capacitive current densities at 0.22 V_{RHE} with different sweep rates of the Cu_2O -D samples.

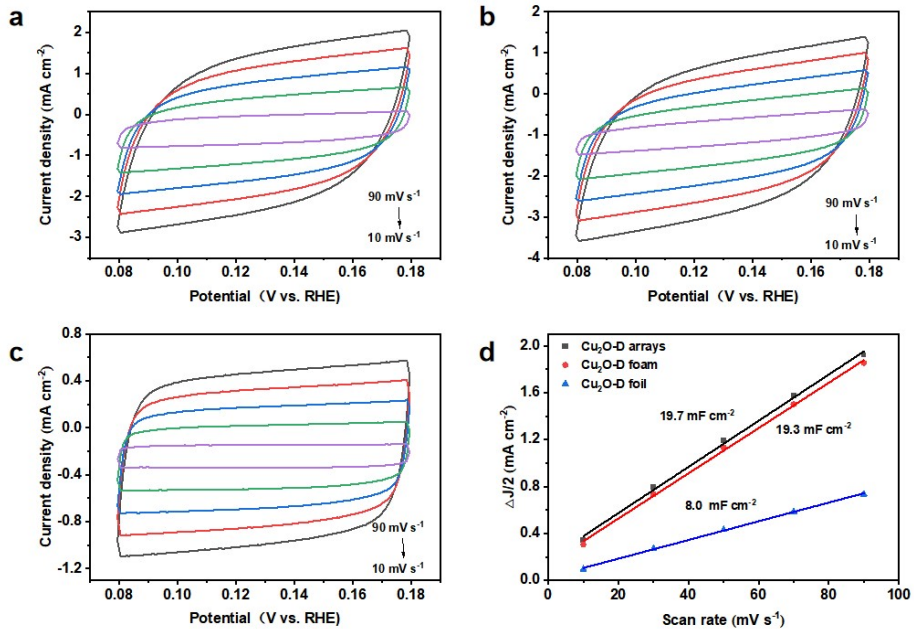


Fig. S9 CV curves of (a) Cu_2O -D arrays, (b) Cu_2O -D foam and (c) Cu_2O -D foil obtained at 0.08–0.18 V_{RHE} with sweep rates from 10 to 90 mV s⁻¹ in pH 9.5. (d) Capacitive current densities at 0.13 V_{RHE} with different sweep rates of the Cu_2O -D samples.

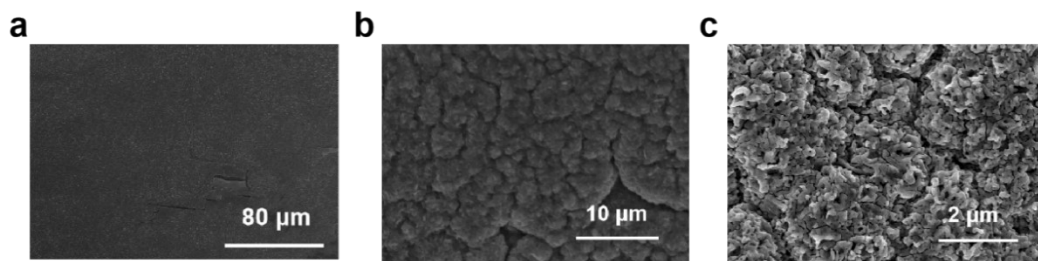


Fig. S10. SEM images of Cu₂O-D foil.

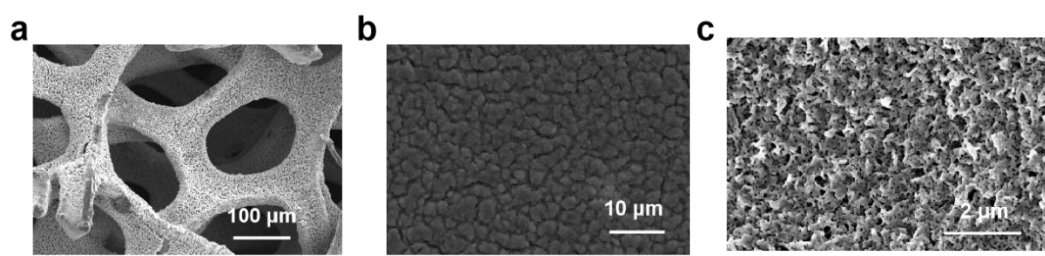


Fig. S11. SEM images of Cu₂O-D foam.

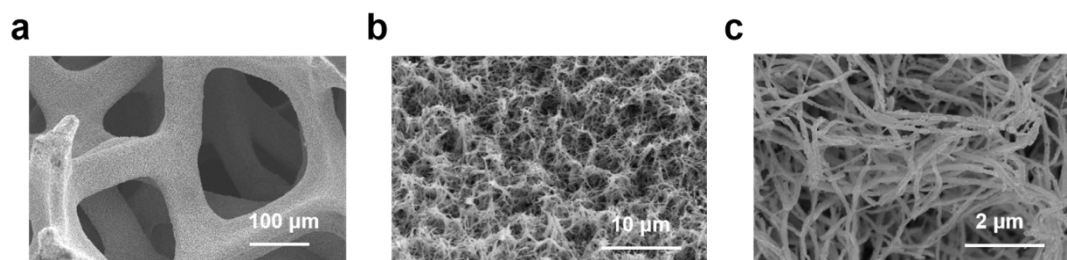
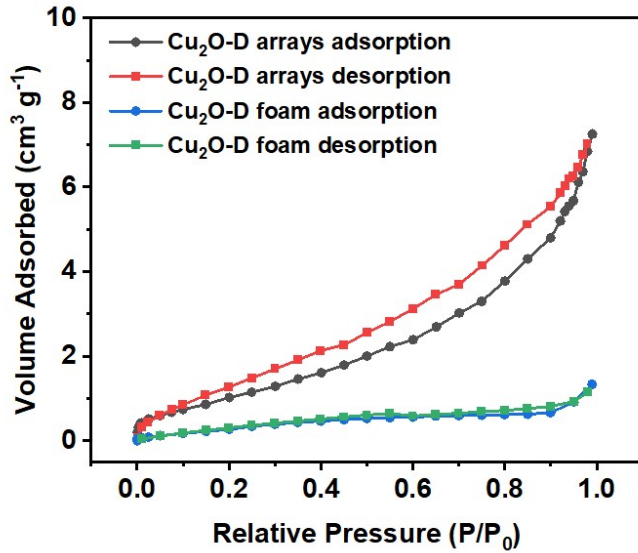


Fig. S12. SEM images of Cu₂O-D arrays.



| | $\text{Cu}_2\text{O-D arrays}$ | $\text{Cu}_2\text{O-D foam}$ |
|--|--------------------------------|------------------------------|
| $a_{s,\text{BET}}$ [m ² g ⁻¹] | 3.73 | 2.54 |
| Total pore volume [cm ³ g ⁻¹] | 8.67×10^{-3} | 6.22×10^{-3} |

Fig. S13. N₂ adsorption/desorption isotherms of the Cu₂O-D arrays and Cu₂O-D foam.

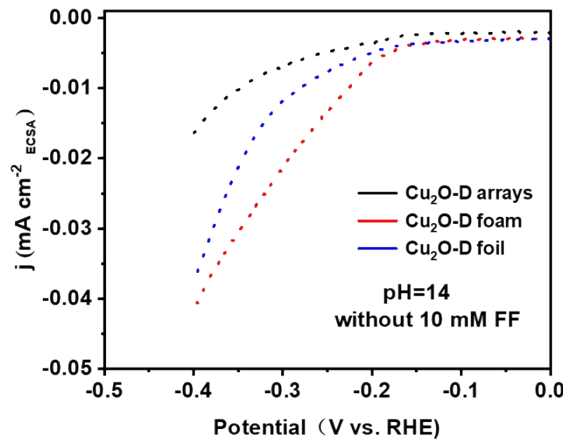


Fig. S14 Current density (in 1.0 M KOH without FF) normalized with ECSA of the Cu₂O-D arrays, Cu₂O-D foam and Cu₂O-D foil.

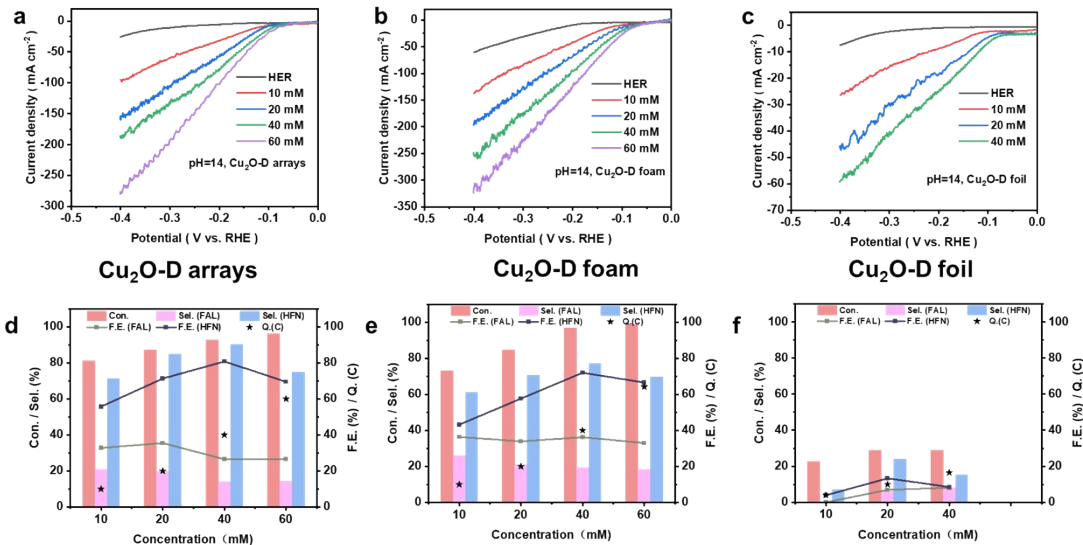


Fig. S15 LSV curves recorded in pH 14 with 10, 20, 40 and 60 mM FF over the (a) Cu₂O-D arrays, (b) Cu₂O-D foam and (c) Cu₂O-D foil. Conversion rate of FF, selectivity and FE to FAL/HFN on (d) Cu₂O-D arrays, (e) Cu₂O-D foam and (f) Cu₂O-D foil in the electrolyte with different FF concentrations.

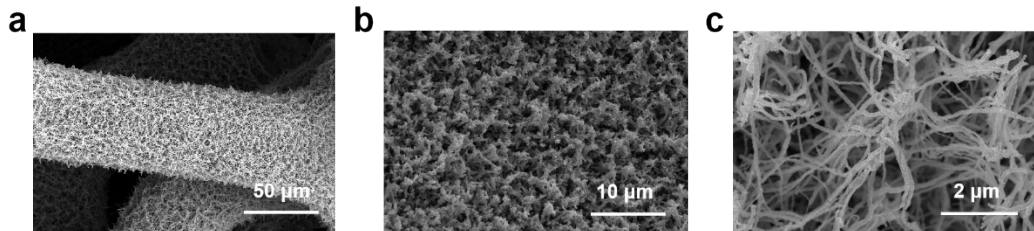


Fig. S16. SEM images of Cu₂O-D arrays after ten cycles.

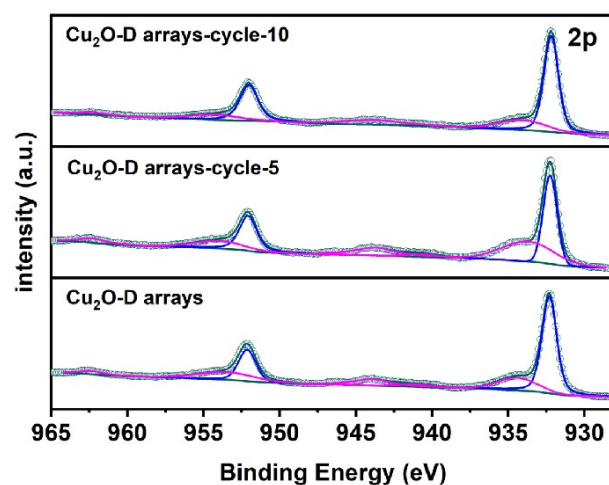


Fig. S17. Cu 2p XPS spectra of the Cu₂O-D arrays after electrocatalytic reduction of FF for five and ten cycles.

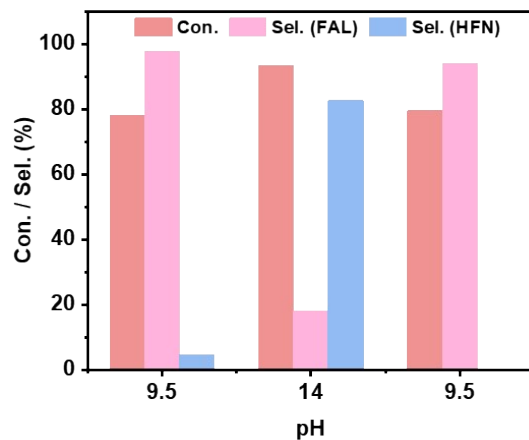


Fig. S18 Conversion rate of FF and selectivity to FAL/HFN on a same Cu₂O-D arrays electrode for electrochemical reduction of FF in the electrolytes with alternate pH between 9.5 and 14.

Table S1 shows the electrolysis conditions and the relevant parameters of the products.

| pH | Potential (V vs. RHE) | Con. (FF)% | Sel. (HFN)% | Sel.(FAL)% | C.B.% | Q.(C) |
|------|-----------------------|------------|-------------|------------|-------|-------|
| 14 | -0.176 | 91.7 | 83.5 | 20.2 | 103.4 | 14 |
| 13 | -0.285 | 95.9 | 65.5 | 35.1 | 100.6 | 19.3 |
| 10.8 | -0.313 | 92.2 | 15.4 | 76.6 | 92.7 | 19.3 |
| 9.5 | -0.341 | 72.1 | 0.5 | 98.4 | 99.3 | 19.3 |

Table S2. A comparison of the performance of electrochemical reduction of FF (HFN production) between the Cu₂O-D arrays and other reported electrocatalysts.

| Catalyst | Potential | pH | Con. | Sel.(HFN) | F.E.(HFN) | Ref. |
|-----------------------------|--------------------|---|---------------|-------------|-----------|--------------|
| Cu ₂ O-D arrays | -0.176 V vs. RHE | 1M KOH (pH 14) | 91.7% | 83.5% | 75.1% | This work |
| Cu-Sn | -0.5 V vs. RHE | 0.1 M phosphate buffer solution (pH6.8) | >97% | >67% | | ¹ |
| Cu/Co doped phthalocyanines | -0.50 V vs. RHE | 0.1 M potassium bicarbonate–carbonate buffer (pH 10) | | | 65.3% | ² |
| 2H-rich MoS ₂ | -1.0 V vs. Ag/AgCl | 0.4 M borate (H ₃ BO ₃ /Na ₂ B ₄ O ₇) buffer in a 1:4 v/v% ratio (methanol:buffer) (pH 9) | 98% | 42.7% | | ³ |
| Cu–NPNi/NF | -0.45 V vs. RHE | 0.5 M NaOH, 50 mM FF | 73.2 ± 2.3% % | 64.2 ± 3.2% | | ⁴ |
| Cu | -1.5 V vs. Ag/AgCl | 0.2 M TBABr+MeCN, containing 5 v/v% H ₂ O. | 51% | >50% | | ⁵ |

Table S3. A comparison of the performance of electrochemical reduction of FF (FAL production) between the Cu₂O-D arrays and other reported electrocatalysts.

| Catalyst | Potential | pH | Con. | Sel.(FAL) | F.E.(FAL) | Ref. |
|----------------------------|--------------------|---|-----------------|-----------------|-----------|-----------|
| Cu ₂ O-D arrays | -0.391 V vs. RHE | 0.1 M Na ₂ CO ₃ -NaHCO ₃ buffer solution (pH 9.5) | 75.4% | 98.4% | 74.1% | This work |
| 15%-Cu/NC900 | -1.3 V vs. Ag/AgCl | 1M KOH (pH 14) | 99% | 99% | 95% | 7 |
| 1T-rich MoS ₂ | -1.2 V vs. Ag/AgCl | 0.4 M borate (H ₃ BO ₃ /Na ₂ B ₄ O ₇) buffer (pH 9) | 98% | 94.4% | | 3 |
| Cu-NPNi/NF | -0.45 V vs. RHE | 0.5 M NaOH, 50 mM FF | 73.2 \pm 2.3% | 21.6 \pm 1.1% | | 4 |
| Cu/Cu-400 nm | -0.5 V vs. RHE | 0.5 M H ₂ SO ₄ | 28.6 \pm 2.8% | 24% | 20% | 8 |
| OP-Cu | -0.56 V vs. RHE | 0.25 M phosphate buffer solution (pH 6.8) | | 96% | 91.1% | 9 |
| Cu ₃ /PC | -0.75 V vs. RHE | acetate buffer (pH = 5) | | | 94% | 10 |
| Ag@Cu NWAs/CF | -0.51V vs. RHE | 0.5 M borate buffer (pH=9.2) | 99.6% | 96.6% | 96.1% | 11 |
| Cu NWAs/CF | -0.51V vs. RHE | 0.5 M borate buffer (pH=9.2) | 88% | 78% | 70% | 11 |

Notes and references

1. X. Liu, Y. Sun, H. Ren, Y. Lin, M. Wu and Z. Li, ACS Catal., 2024, 14, 5817-5826.
2. Z. Mukadam, S. Liu, A. Pedersen, J. Barrio, S. Fearn, S. C. Sarma, M.-M. Titirici, S. B. Scott, I. E. L. Stephens, K. Chan and S. Mezzavilla, Energy Environ. Sci., 2023, 16, 2934-2944.
3. S. Huang, B. Gong, Y. Jin, P. H. L. Sit and J. C.-H. Lam, ACS Catal., 2022, 12, 11340-11354.
4. R. J. Dixit, K. Bhattacharyya, V. K. Ramani and S. Basu, Green Chem., 2021, 23, 4201-4212.
5. M. Temnikova, J. Medvedev, X. Medvedeva, N. H. Delva, E. Khairullina, E. Krivoshapkina and A. Klinkova, ChemElectroChem, 2022, 10, e202200865.
6. X. Shang, Y. Yang and Y. Sun, Green Chem., 2020, 22, 5395-5401.
7. W. Xu, C. Yu, J. Chen and Z. Liu, Appl. Catal. B-Environ., 2022, 305, 121062.
8. S. Jung, A. N. Karaiskakis and E. J. Biddinger, Catal. Today, 2019, 323, 26-34.
9. P. Chen, W. Zhang, J. Tan, Y. Yang, Y. Jia, Y. Tang and Q. Gao, Catalysis Science & Technology, 2022, 12, 4032-4039.
10. P. Zhou, Y. Chen, P. Luan, X. Zhang, Z. Yuan, S.-X. Guo, Q. Gu, B. Johannessen, M. Mollah, A. L. Chaffee, D. R. Turner and J. Zhang, Green Chem., 2021, 23, 3028-3038.
11. Y. Zhong, R. Ren, Y. Peng, J. Wang, X. Ren, Q. Li and Y. Fan, Mol. Catal., 2022, 528, 112487.